Carbon-Based Nanostructures for Matrix-Free Mass Spectrometry

Yannick Coffinier, Rabah Boukherroub and Sabine Szunerits

Abstract Matrix-assisted laser desorption/ionization mass spectrometry (MALDI-MS) has become a widespread analytical tool for peptides, proteins and most other biomolecules. However, due to a competitive desorption of parasitic ions from the matrix, it is difficult to detect low molecular weight compounds (<700 Da). To enable desorption/ionization of small molecules, techniques operating in absence of an organic matrix were developed. These techniques known as surface assisted laser desorption/ionization mass spectrometry (SALDI-MS) rely on the use of nanostructured surfaces as laser desorption/ionization-assisted material. As compared to traditional MALDI-MS, SALDI-MS offers several advantages such as the ability to detect small molecules (<700 Da), easy sample preparation, low noise background, high salt tolerance and fast data collection. Carbon-based interfaces such as carbon-like graphite, carbon nanotubes, fullerenes or amorphous carbon have been employed as SALDI substrates for the detection of small macromolecules such as synthetic polymers and biomolecules. While the drawback of fullerenes and their derivatives is the general limited sensitivity, carbon nanotubes, which exhibit high sensitivities, are hardly soluble in aqueous solutions, limiting their use in bioanalytical applications. More recently, diamond-like carbon (DLC) and diamond nanowires have been successfully introduced as SALDI interfaces. This chapter summarizes recent developments in the use of carbon-based materials for SALDI-MS. A particular emphasis will be put on the use of diamond nanowires as novel SALDI substrates.

Keywords Surface assisted laser desorption/ionization mass spectrometry (SALDI-MS) · Carbon-based nanostructures · Diamond nanowires · Small molecules · Biomolecules

Y. Coffinier · R. Boukherroub · S. Szunerits (✉)
Institut d'Electronique, de Microélectronique et de Nanotechnologie (IEMN, UMR 8520), Cité Scientifique, Avenue Poincaré, B.P. 60069, 59652 Villeneuve d'Ascq, France
e-mail: sabine.szunerits@iri.univ-lille1.fr

N. Yang et al. (eds.), *Carbon Nanoparticles and Nanostructures*, Carbon Nanostructures, DOI 10.1007/978-3-319-28782-9_10

1 Introduction

Mass spectrometry (MS) is widely accepted as a 'gold-standard' method for identifying chemicals or biological products. It is nowadays applied in highly diversified domains like those directly or indirectly tied to healthcare or regulation-driven demand, such as drug development, diagnostics, food and environmental safety testing. Among the different methodologies, matrix-assisted laser desorption/ionization mass spectrometry (MALDI-MS), first introduced in 1988 by Hillenkampf and Karas [1], constitutes one of the soft ionization techniques that provides the nondestructive vaporization and ionization of analytes using UV-absorbing organic matrices. The utility of MALDI-MS for protein and peptide analysis lies in its ability to provide high accurate molecular-weight information on intact molecules. Acquiring optimum MALDI data depends not only on the functional and structural properties of the analyte itself, but also largely on the choice of suitable matrices. As the matrix is the medium by which the analyte is transported to the gaseous phase and provides the conditions that make ionization possible, the matrix and the sample-matrix preparation procedure greatly influence the quality of MALDI mass spectra. Organic matrices such as 2,5-dihydroxylbenzoic acid, α-cyano-4-hydroxycinnamic acid or 3,5-dimethoxy-4-hydroxycinnamic acid are commonly used. However, the choice of the matrix remains an empirical issue. Although MALDI-MS has been successfully used to analyze large molecules [2–4], it has rarely been applied to low-molecular weight compounds (<700 Da) as a large number of matrix ions appear in the low-mass range.

Using inorganic species as the assisting material in MALDI-MS is an alternative approach to avoid the problems arising in conventional MALDI analysis using organic compounds as matrix systems. Tanaka et al. [5] investigated a suspension of cobalt nanoparticles of 30 nm in size mixed with glycerol as inorganic matrix for the laser desorption/ionization of small analytes. Since then, several alternative inorganic matrices have been proposed as assisting materials [6] in a process that was named surface assisted laser desorption/ionization mass spectrometry (SALDI-MS) by Sunner et al. [7]. The basic principle of SALDI-MS analysis is schematically outlined in Fig. 1. Two different approaches are currently used. One, a true matrix-free approach, is based on the deposition of the analyte solution on a nanostructured surface, previously deposited on MALDI-plate (Fig. 1a). The other approach uses a mixture of the analyte together with SALDI nanostructures for analysis (Fig. 1b). There are indeed several advantages associated with inorganic matrix systems for MALDI-MS analysis, such as the elimination of co-crystallization of the sample with an organic matrix, limiting formation of hot spots. Moreover, the absence of peaks from the matrix in the low mass range encountered in classical MALDI-MS allows increasing the background of the spectra and lowering the sensitivity of detection of small molecules.

One of the most notable developments in the use of solid interfaces as matrix for LDI-MS has certainly been desorption/ionization on porous silicon [8] (DIOS) for the analysis of low molecular mass compounds. Porous silicon substrates are easily

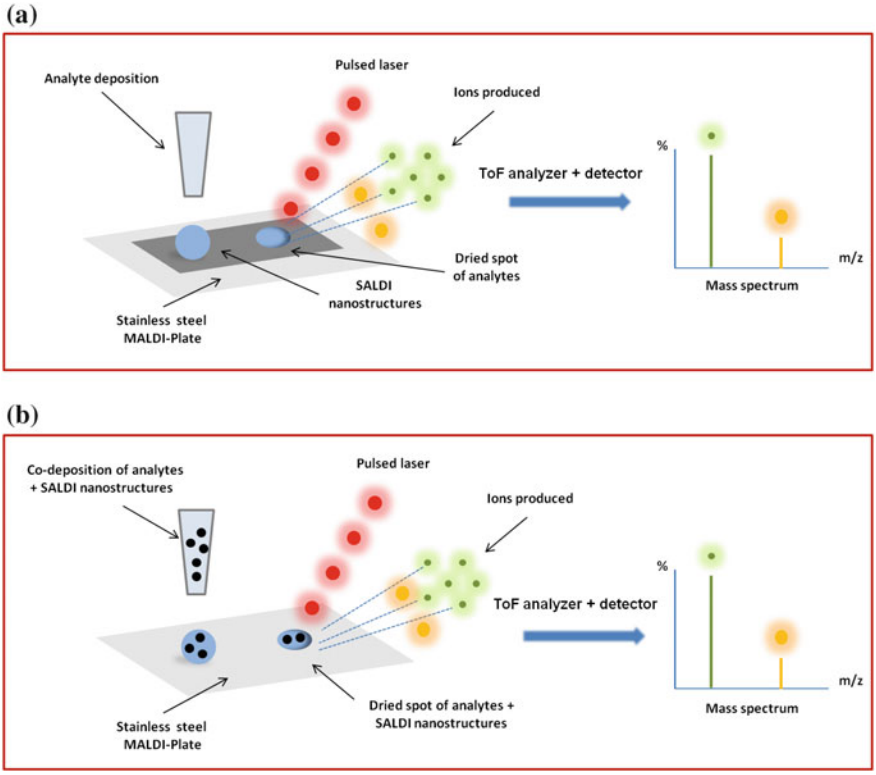

Fig. 1 Schematic presentation of the principle of surface assisted laser desorption/ionization mass spectrometry (SALDI-MS): LDI-MS process for analyte detection with analyte deposition on SALDI based nanostructures (**a**), and co-deposition of analyte and SALDI-based material (**b**)

obtained by electrochemical anodization of crystalline silicon in HF-based solutions. Using the same mass spectrometer as for MALDI (i.e. N_2 laser $\lambda = 327$ nm and time-of-flight (TOF) analyzer), an optimal performance for molecules less than 3 kDa was achieved [9]. It is believed that the low thermal conductivity of porous silicon confines heat close to the surface, thus increasing locally the temperature and resulting in sensitivities exceeding those of classical MALDI-MS [10]. Furthermore, by using silicon nanowires rather than porous silicon allowed to decrease the laser irradiation energy required for analyte desorption, resulting in an extremely gentle ionization process [11, 12] for SALDI-MS.

Along with nanostructured silicon, other semiconductors with good UV absorbance are in addition promising candidates for SALDI-MS [6]. The large number of nanomaterials, together with different preparation techniques, make classification into well-defined LDI categories and distinguishing it from MALDI somewhat difficult. This situation is not helped by the large number of different acronyms that are currently used for SALDI-MS, many of which describe similar or essentially the same methodologies. For instance, PALDI is referred as Particles-Assisted Laser

Desorption/Ionization, but also as Polymer-Assisted Laser Desorption/Ionization. Another point is that some researchers consider SALDI as a matrix-free technique, whereas others consider it as MALDI using an inorganic matrix. To avoid the multiplication of acronyms, we prefer classification of SALDI-based matrices upon their chemical composition. Like this, three main groups emerge as SALDI candidates [13]: (i) semiconductor-based, (ii) metal and metal-oxide based and (iii) carbon-based SALDI structures.

In the case of carbon-based matrices, this classification scheme is, however, highly insufficient, as carbon can range from being a pure insulator (diamond) over a semiconductor (semiconducting nanotubes) to a metal (metal nanotubes and graphite) [14]. Furthermore, carbon atoms can be arranged into different crystal structures revealing different physical and chemical properties. The sp^2 hybridized carbon structures such as graphite, carbon nanotubes (CNTs), fullerenes or graphene have been reported to be effective matrices for SALDI-MS [15–23].

On the other hand, sp^3 hybridized carbon in the form of diamond particles and wires have also shown lately to be useful SALDI substrates [24]. With its exceedingly high bulk modulus and hardness, diamond has historically been considered as the hardest material available. Although diamond is a wide band gap semiconductor, diamond can be easily doped, particularly with boron atoms to prepare highly conductive boron-doped diamond (BDD) films. BDD has been recognized as one of the most promising electrode material for electrochemical applications, because of its unique features such as wide potential window and negligible capacitive current. Consequently, BDD electrodes have been investigated for a wide range of electrochemical applications [25, 26]. The analytical performance of BDD-based biosensors was considerably improved by increasing the surface area through structuring BDD interfaces into nanowires [27–30]. Luo et al. [31] showed that diamond nanoforest electrodes are electrochemically active towards glucose sensing under basic conditions. The importance of the diamond nanowires' length for the non-enzymatic detection of glucose was recently underlined by our group [32]. The electrochemical activity of 3 μm long diamond nanowires is 3.5 times larger compared to as-grown planar BDD electrode and 2.4 times higher than 1 μm long diamond nanowires resulting in increased sensitivity to glucose [32]. Such diamond nanowires proved to be also an excellent electrical interface for the detection of tryptophan and/or tyrosine, two aromatic acids that are important precursors for adrenaline, dopamine or melatonine [32–34]. Next to these examples where the intrinsic properties of diamond nanowires were exploited for sensitive and selective sensing, polymer [35] and metallic nanoparticles coated diamond nanowires [30, 36, 37] have shown additional interest for electrochemical sensing.

While the use of diamond nanowires electrodes for electrochemical sensing has been recently reviewed [38], the intent of this article is to make the reader more familiar with recent developments for the preparation of diamond nanostructures and the use of such structures as LDI-MS surfaces. To put the work on diamond nanowires into perspective, first, the current state of the art on carbon-based nanomaterials such as graphite and carbon nanotubes (CNTs), for the detection of

analytes by LDI-MS will be described. Thereafter, the synthetic routes for diamond nanowires and their use as SALDI-MS substrates will be presented around some pertinent examples.

2 Carbon-Based Materials for SALDI

Carbon-based nanomaterials can been considered ideal SALDI-MS matrices. They provide high-affinity binding sites for peptides and proteins by virtue of their chemical functionalities where hydrophobic and hydrophilic forces are taking place. To minimize probable contamination from these materials due to ionization, extended surface modification strategies can be adopted to decrease the tendency to fly off into the instrument when a laser pulse was applied. This chemical diversity together with remarkable charge mobility and universal optical absorption properties make carbon-based structures the focus for SALDI (Table 1).

Table 1 Carbon-based materials for LDI-MS

Carbon material	Analysis	Comments	References
Colloidal graphite	Fatty acids, flavonoids (negative mode, fmolar range)		[47]
Colloidal graphite	Peptides and proteins		[7]
Colloidal graphite aerosols	Different small molecules (fatty acid, carbohydrates, flavonoids, phospholipids, etc.)	In isopropyl alcohol	[45–47]
Activated carbon	Peptides and proteins	Deposited on TLC plates	[39]
Graphite plate	Polymers, fatty acid		[40–42]
Pencil line	Peptides	On silica gel matrix	[44]
Pyrolitic graphite sheet (PGS)	Environmental related compounds (e.g. bisphenol A, 4-choloraniline, etc.)		[48]
CNTs	Peptides and proteins profiling	Derivatized with iminodiacetic acid (IDA), and loaded with copper	[49]
CNTs-citric acid	selective capture of positively charged species such as cytochrome c	Citric acid-treated	[50]
Oxidized CNTs	Amino acids, small molecules, oligosaccharides		[22, 23, 53]
CNTS	Amino acids		[54]
CNTs	Herbal components		[59, 60]

(continued)

Table 1 (continued)

Carbon material	Analysis	Comments	References
Oxidized CNTs	Organotin, organoarsenic, organophosphate, organomercury, alkyl phenol, anilines, atrazine derivatives, naphthol derivatives, chlormequat chloride, diquat, paraquat, humic acid, and decabromodiphenyl oxide		[61]
Oxidized CNTs	Amino acids, Jatrorrhizine		[62]
SWNTs	Peptides	$(CH_2)_2COOH$ modified	[21]
Fullerenes	Proteins		[56]
Fullerenes	Proteins	Hexa(sulfonbutyl) modified	[15]
Fullerenes	N-terminal sulfonated peptides	N-dimethyl pyrrolidinium iodide modified	[57]
Fullerenes	Peptides	$(CH_2)_2COOH$ modified	[21]
Fullerenes	Proteins	Modified	[58]
Diamond particles	Albumin, myoglobin, cytochrome C	Presence of HCCA	[63]
Nanocrystalline diamond (NCD)	Protein profiling	Activation by glycidyl methacrylate and introduction of IDA-Cu^{2+} complex	[64]
Diamond nanocrystals (100 nm diam.)	Solid phase extraction of DNA and MS detection	Poly-lysine coating on carboxylated diamond nanocrystals	[65]
Diamond nanowires	Peptides, verapamil (zeptomole range of detection), cortisone	Octadecyl-terminated	[24]

2.1 Graphite

Graphite particles were the first carbon-based materials introduced as SALDI-MS matrix [7]. Laser desorption/ionization time-of-flight (TOF) mass spectra of peptides and proteins, as well as low molecular weight analytes, could be obtained by using a pulsed UV laser (337 nm) to irradiate mixtures of 2–150 μm graphite particles and solutions of the analytes in glycerol (Fig. 2a). At optimum conditions, mass spectra with signal intensities as good as those in conventional MALDI with very few background peaks, even at low mass were obtained. For example, Fig. 2a shows the low-mass region of a graphite SALDI spectrum of glycerol. The ion at m/z = 93 is protonated glycerol. This ion and the fragments at m/z = 75, 57, 45, 29 and 19 are all prominent in the spectrum. The other fragments are due to alkali salt impurities and alkali ions/glycerol adducts. A series of peaks due to carbon clusters,

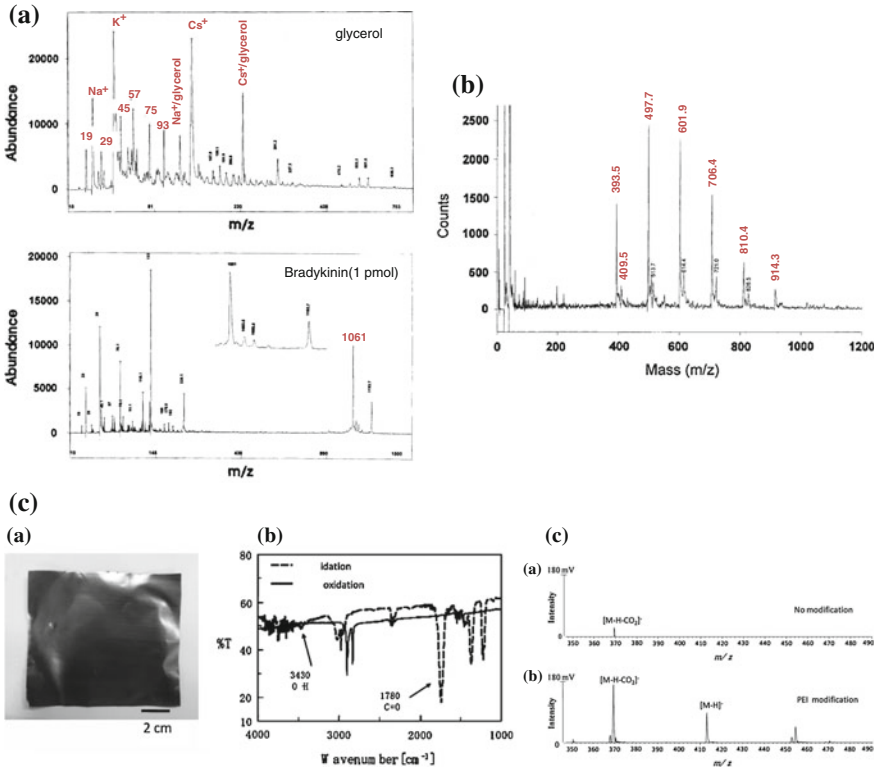

Fig. 2 **a** Graphite SALDI of glycerol and Bradykinin (reprint with permission [7]). **b** Graphite plate assisted SALDI-MS analysis of low-mass polystyrene by depositing 1 μL (1 mg/mL) of the polymer sample on the graphite plate without additional matrix (reprint with permission from [40]). **c** Image of pyrolitic graphite sheet (PGS) (*a*) together with FT-IR ATR spectrum and (*c*) Mass spectrum of PFPA using non-modified and PEI-modified PGS in negative ion mode. The sample concentration was 0.1 mg/ml (reprint with permission from [48])

$C_nH_m^+$ with n = 1–25 and beyond, and m = 0–4 are observed, being low in intensity. The technique was also suitable for the analysis of biomolecules such as bradykinin in glycerol (1 pmol).

The same group further developed activated carbon particles deposited on thin-layer chromatography (TLC) plates and used them for SALDI-MS analysis [39]. Indeed, one of the advantages of graphite is that it can be used either in solution (graphite/liquid mixture) or as dry graphite (without liquid). Kim et al. [40] investigated, for example, a graphite plate as substrate and matrix for the SALDI-MS detection of polystyrene and poly(methylsilsesquioxane) (PMSSQ) materials derived from methyltriethoxysilane (MTES) in the range of 100–1000 Da. Figure 2b shows a graphite plate SALDI mass spectrum of a polystyrene standard in the low mass range. The styrene oligomers were separated by 104.3 mass units, related to $[(C_6H_5)CHCH_2]$ repeat units. The peak at m/z = 393.5 is the

sodium adduct of styrene trimer with *tert*-butyl and hydrogen at the ends and the peak at m/z = 409.5 is evident of the potassium adduct [40]. By using the same home-made graphite plate, they were also able to detect underivatized fatty acid extracted from alkaline hydrolysis of triglycerides or from food (milk and corn oil) and from phosphatidylcholine [41]. Graphite plates in combination with glycerol showed also to be useful for the identification of synthetic polymers and biological molecules using visible LDI-MS (532 nm laser) [42], offering a soft ionization procedure over UV-based SALDI-MS.

The feasibility of directly obtaining analyte signals from a planar silica gel surface by SALDI-MS was demonstrated by Chen and Wu [43]. A pencil line of ≈1 mm in width was drawn onto a silica gel surface of a TLC plate, over which a liquid matrix (15 % sucrose/glycerol–methanol 1:1 v/v) with the analyte was applied. The laser was then used to directly irradiate the sample spot on the pencil line. One of the crucial advantages is that the carbon deposition by this method resulted in more homogenous matrices than by applying a suspension of carbon powder mixed with a liquid matrix on the silica gel surface [44]. This pencil matrix was thus considered for a long time as an inexpensive, quick, and easy-to-use matrix providing optimum results for SALDI analysis.

Commercial colloidal graphite aerosol sprays, containing colloidal graphite suspension in isopropylic alcohol were proposed by Cha and co-workers for the fabrication of carbon matrices on stainless steel plates [45–47]. The group of Zhang used these carbon matrices for the detection, localization and identification of various small compounds such as phospholipids from rat brain tissue (slice) [45], metabolites (fatty acid, flavonoïds, carbohydrates) from fruit slices [47] and flavonoïds from plant tissue wax [46].

Highly oriented graphite film known under the name Pyrolitic Graphite Sheet (PGS) has been employed by Kawasaki to analyze low-mass analytes by SALDI-MS [48]. PGS is a synthetic, uniform and highly oriented graphite polymer film that provides thermal management/heat-sinking in limited spaces (Fig. 2c). It shows high thermal conductivity (600–1500 Wm^{-1} K), being twice that of copper and ten times of ordinary graphite. The large heat conduction anisotropy of PGS allowed the rapid heating of the PGS surface by the laser radiation, which is crucial for efficient LDI-MS. Various environmentally related compounds (e.g. bisphenol A, 4-chloroaniline, perfluorooctanoic acid (PFOA), etc.) were detected using this approach [48]. The influence of surface modification of PGS on the signal intensity for perfluorooctanoic acid (PFOA) analysis was in addition demonstrated (Fig. 2c). The signal intensity of PFOA detected on PGS modified with polyethyleneimine (PEI) showed a ten-fold increase over that obtained from desorption/ionization on porous silicon (DIOS), the reference SALDI surface. PFOA could be quantified using SALDI and a wide linear dynamic range response from 20 to 1000 ppb was observed [48]. The advantages of PGS as SALDI matrix are therefore linked to the large film morphology of the PGS, that low volume of analyte solution can be directly deposited onto PGS, resulting in good reproducibility of intra and inter-sample spots, making quantitative analysis possible. Surface modification of the PGS is in addition easy and various functionalized surfaces to concentrate target

analytes can be obtained. All these features make PGS a suitable material for the LDI-MS of small molecules.

2.2 Carbon Nanotubes (CNTs)

The development of reliable methods for the fabrication of carbon nanotubes (CNTs) has enabled the use of this material in SALDI-MS analysis [14, 18, 49, 50]. Wang and co-workers showed that CNTs of 250 nm in diameter and ca. 60 μm in length, which can disperse very well in solution, can be employed as SALDI matrix [51] (Fig. 3a). The same group reported a year later, that adding a citrate buffer provides an extra proton-source and also reduced the intensities of sodium adduct ions of analytes during SALDI-MS analysis [52]. As the surface of CNTs can be easily modified in numerous ways, they formed anionic CNTs through immersion into citric acid and used the treated CNTs as affinity probes for the selective capture of positively charged species [50]. The potential of citrate-treated CNTs was demonstrated through the detection of very low concentrations of insulin. The pI value of insulin is 5.3 and thus it has a net positive charge in solutions at pH 4. Figure 3a displays the SALDI-MS spectra of insulin solution (10^{-8} M) at pH 4 and pH 10. The protonated pseudomolecular ion of insulin (MH^+) at m/z = 5734 dominates the spectrum at pH 4, while no insulin peak was detected at pH 10 [50]. Cytochrome c with a molecular weight of 1–12 kDa is the largest molecule detected by this technique.

Oxidized CNTs have been widely tested as matrix substance for the analysis of small molecules by SALDI-MS. Oxidized CNTs allowed for example the analysis of mixtures of amino acids containing Asn, Glu, His, and Phe [22]. As shown in Fig. 3b, mass spectra of these amino acids using CNTs and oxidized CNTs as matrix substrates displayed well-separated peaks as $[M + H]^+$, $[M + Na]^+$ and $[M + K]^+$. Intensity and S/N ratios were considerably improved for the oxidized CNTs matrix compared to simple CNTs due to the removal of many impurities during the oxidation procedure together with its better dispersibility in water (Fig. 3a). Pan et al. [53] developed in addition an approach where CNTs served both as the adsorbent in solid-phase extraction and as matrix for LDI-MS analysis for small molecules (β-Arg, N-Alpha-Benzoyl-L-Arginine ester ethyl (BAEE), propranolol, and Leu-Tyr) in solution. The detection limit for analytes could be improved 10- to 100-fold with this approach. Subsequently, twenty common amino acids have been analyzed by LDI-MS by Zhang et al. [54]. The mass spectra of a mixture of seven amino acids, including Phe, Trp, Tyr, Leu, Ile, Val, and Met, showed good signals with small intermolecular interferences. Leu and Ile were not differentiated because of similar molecular weights, whereas a detection limit of 6 pmol was achieved [54].

Next to CNTs, single-walled carbon nanotubes (SWNTs) modified with $-(CH_2)_2COOH$ groups were proposed by Ugarov et al. for the analysis of peptide solutions by SALDI-MS [21]. The authors showed that the position of acidic

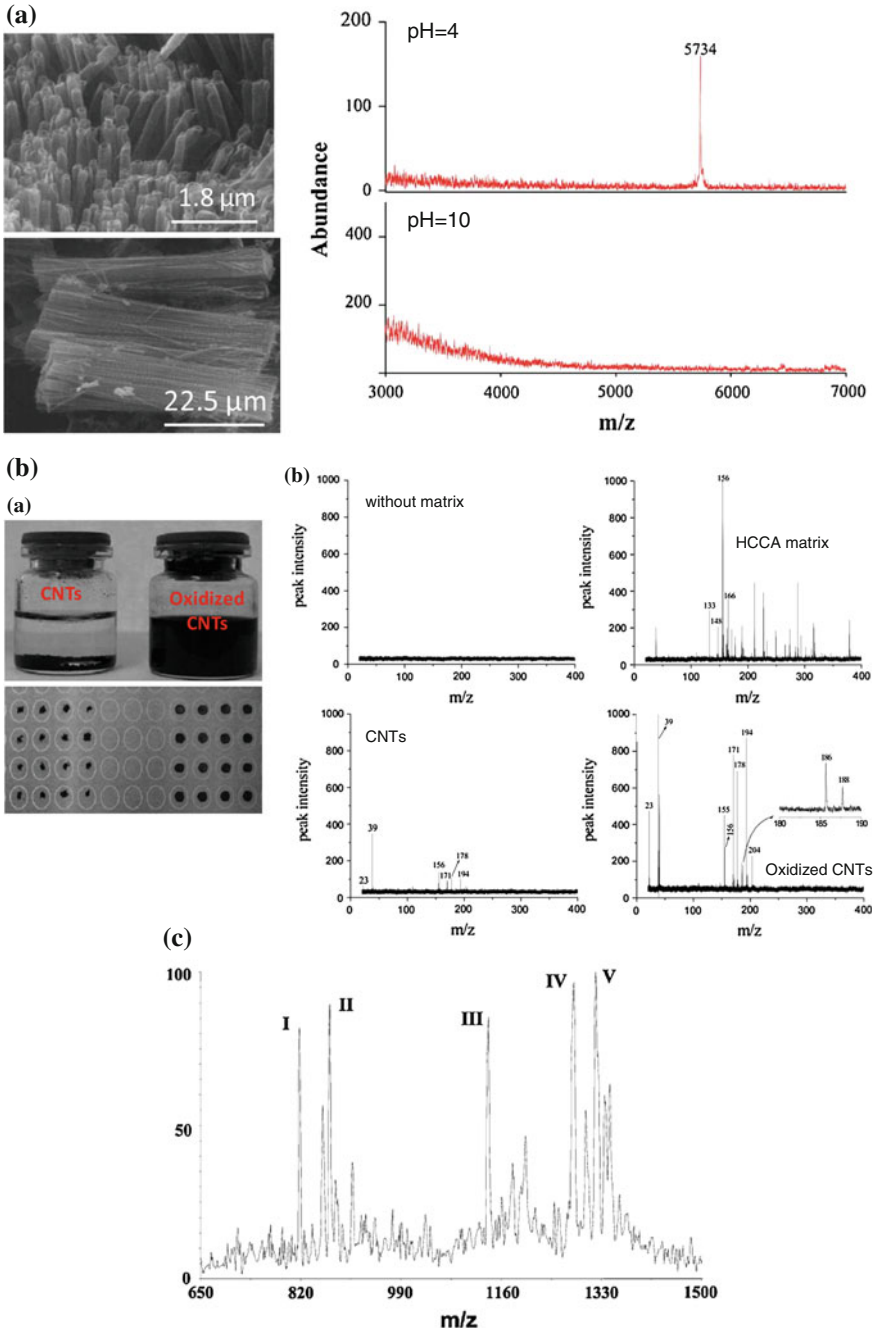
(a)
1.8 µm
22.5 µm
pH=4
5734
pH=10
Abundance
m/z
(b)
(a)
CNTs
Oxidized CNTs
(b)
without matrix
HCCA matrix
CNTs
Oxidized CNTs
peak intensity
m/z
(c)
I
II
III
IV
V
m/z

◀ **Fig. 3** **a** SEM images of CNTs and SALDI-MS spectra of insulin obtained using citrate-treated CNTs as affinity probes to trap insulin from sample solutions containing 10^{-8} M insulin at pH 4 and pH 10 (reprint with permission from [50]). **b** (*a*) Comparison of solubility of CNTs and oxidized CNTs in water and matrix layers of CNTs and oxidized CNTs, (*b*) Mass spectra for 4 amino acid mixture solutions containing Asn, Clu, His and Phe in the LDI mode without matrix, and with HCCA matrix, CNTs and oxidized CNTs (reprint with permission from [22]). **c** SALDI spectrum of 4 peptides at femtomolar loading. *I* RRPYIL (81,800 amu), *II* dynorphon 1–7 YGGFLRR (868.0 amu), *III* dynorphin 1–9 YGGFLRRIR (1138.4 amu); and *IV* goosefish angiotensin I NRVYVHPFHL (1281.5 amu). The concentration of each peptide was 25 fmol/μL (water solution) (reprint with permission from [21])

moieties on the walls of nanotubes is essential for SALDI analysis. Indeed, CNTs with the functional groups attached to the ends do not work as LDI-MS matrices, which means that the attachment to the walls is critical for desorption/ionization. Four peptides (RRPYIL (818.0 amu), dynorphin 1–7 YGGFLRR (868.0 amu), dynorphin 1–9 YGGFLRRIR (1138.4 amu), and goosefish angiotensin I NRVYVHPFHL (1281.5 amu) were efficiently detected with this system at femtomole concentrations [21] as seen in Fig. 3c.

2.3 *Fullerenes*

The discovery of buckminster fullerene (C_{60}) together with its subsequent large-scale synthesis have initiated a growing research field in the area of biochemistry and life sciences using this material [55]. Hopwood was one of the first considering C_{60} as LDI matrix [56]. In that case, the analytes were deposited on a pre-deposited thin film (10 nm) of fullerenes and measured the positive ions generated with a nitrogen laser. Although some proteins, such as Cytochrome C (12 kDa) and bovine serum albumin (BSA, 66 kDa), are detected by this method, the sensitivity is still lower than with organic acids as matrix. The reason for this lower sensitivity may be the uneven dispersion of polar analytes in the non-polar fullerene matrix.

To overcome this problem, a water-soluble fullerene derivative, hexa(sulfonbutyl)fullerene $C_{60}[(CH_2)SO_3^-]_6$ (HSBF) was synthesized [15]. HSBF consisted of a C_{60} cage, covalently bonded with six negatively charged sulphonate arms (Fig. 4a). This matrix was used as an ion-parting reagent to precipitate analytes in a mixture, depending upon the charge, structure, and hydrophobic character of each analyte [15]. As HSBF shows strong optical absorbance in the UV range, no additional organic matrix was required to conduct SALDI-MS analysis. The affinity of various proteins to HSBF was studied by the authors [15]. For example, digestion of myoglobin with trypsin generated peptides that are positively charged and the peptides in abundant quantity suppress the signals of some important trace peptides, which were quite evident on precipitation by HSBF, due to strong affinity of the fullerene derivative to lysine ends of these peptides (Fig. 4a).

Other fullerene modifications such as the *N*-dimethyl pyrrolidinium iodide modified fullerene allowed the enrichment of N-terminal sulfonated peptides [57]. In parallel to the work on SWNTs, Ugarov demonstrated the interest of acid-terminated fullerenes [C_{60} $(CH_2)_2COOH)_n$] as matrix material for LDI-MS analysis of a solution of 4 peptides [21]. Due to the presence of acidic groups, no additional components are needed for decreasing the pH and perform an effective ionization. Vallant et al. [58] showed that fullerene-based materials with different chemical moieties can be successfully employed for selective enrichment and identification of low mass serum constituents. Dioctadecyl methano fullerenes, fullerenoacetic acid and iminoacetic acid (IDA)-fullerenes were prepared (Fig. 4b) and subjected to a comprehensive characterization study including protein binding properties and capacity. Indeed, in this study a new strategy was elaborated enabling both screening of biological samples using SALDI and identification of serum constituents in a broad mass range (m/z = 1000–30,000) after elution of bound analytes as seen in Fig. 4b. It has been shown that diverse functionalities result in characteristic human serum patterns in terms of signal intensity as well as the number of detectable masses (Fig. 4b). As depicted in Figs. 4b, the carboxylated fullerenes provided a number of signals, whereas the more hydrophobic dioactadecyl methano fullerene was characterized by a total absence of expedient

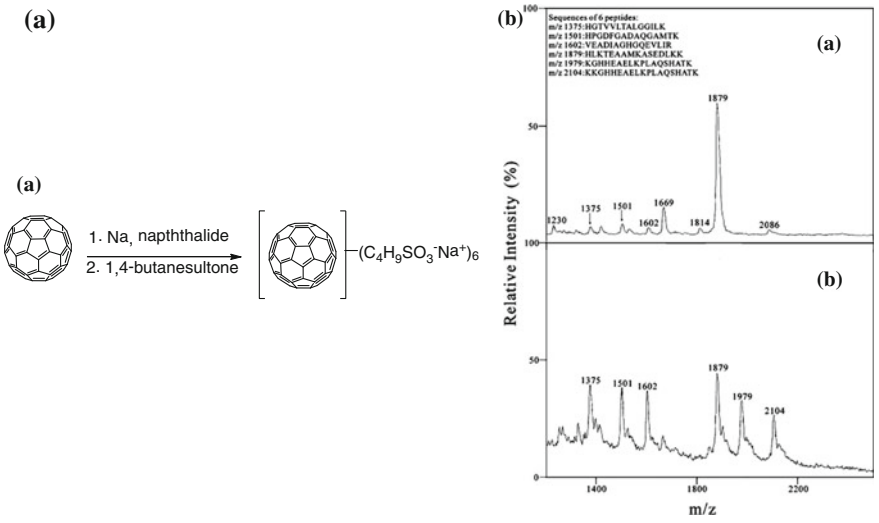

Fig. 4 **a** (*a*) Synthetic procedure of the sodium salt water soluble fullerene derivative hexa (sulfonbutyl)fullerene $C_{60}[(CH_2)SO_3^-]_6$ (HSBF), (*b*) SALDI spectrum of the trypsin-digested myoglobulin solution (1 mM) with particle LDI mass spectrum; **b** (*a*) different fullerene derivatives used for LDI-MS, (*b*) representation of low molecular mass working flow of human serum enriched on derivatized fullerenes: (*A*–*C*) fullereneacetic acid, (*D*–*F*) dioctadecyl methanofullerene: *A* + *D* MALDI spectra, *B* + *C* MALDI before MC-separation, *C* + *F* MALDI after liquid chromatography separation and fractionation (reprint with permission from [58])

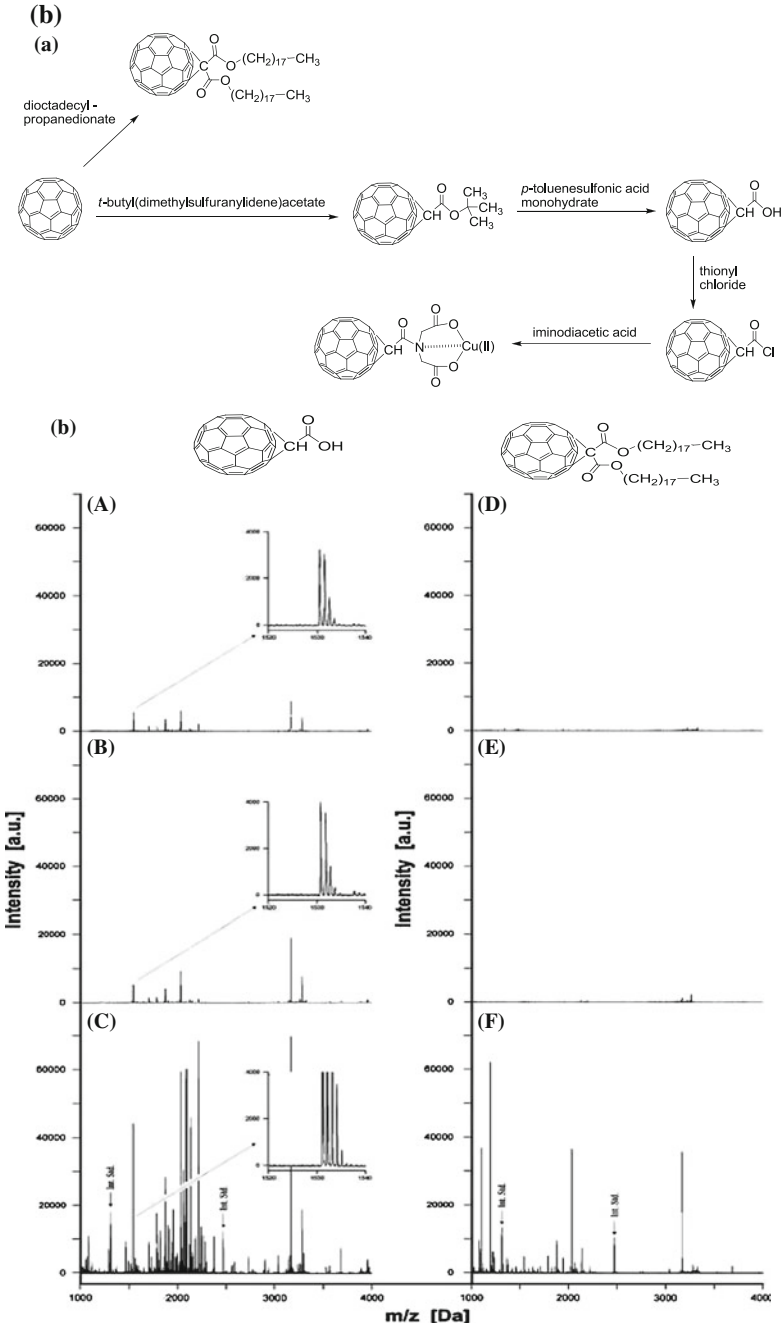

Fig. 4 (continued)

masses. However, the intensity and resolution of the peptide mass signals, based on direct irradiation of the SALDI support were found to be too low for reasonable analysis. For a more comprehensive study of lower mass serum constituents, adsorbed components were eluted from the derivatized fullerenes, showing increased signal intensity.

2.4 Diamond-Based Structures

Next to sp^2-based carbon materials, sp^3 carbon allotropes have also been investigated as inorganic matrices for SALDI-MS.

2.4.1 Diamond-like Carbon (DLC)

The group of Bonn has examined for the first time, the use of diamond-like carbon (DLC), an amorphous material with various levels of sp^3 and sp^2 hybridized carbons, for LDI-MS detection of metabolites and low-molecular weight peptides [14]. DLC films were deposited onto molybdenum-sputtered "digital versatile disc" (DVD) (Fig. 5a). The advantage of using DVDs as a base material is related to the possibility to save mass data directly onto the disk. DLC coating with 35 % sp^3 carbon content and a thickness of approximately 300 nm was prepared by pulsed laser deposition (PLD) technique, providing fast deposition rates and homogeneous DLC coatings. The nanostructures (nanogrooves) were achieved either through chemical or laser etching and showed maximum absorption between 305 and 330 nm (nitrogen laser, 337 nm). The detection of different analytes like amino acids, carbohydrates, lipids, peptides was achieved with such interfaces [14] (Fig. 5b–d). The detection limits for [Glu^1]-fibrinopeptide B (m/z 1570.6) and L-sorbose (Na^+ adduct) were for example 10 and 1 fmol/μL, respectively. One of the major advantages is that the device does not require any chemical functionalization and DLC provided longer lifetimes without any deterioration in the detection sensitivity [14, 66]. However, this type of device needs to be adapted to commercial mass spectrometer. To overcome this problem, Winkler et al. have deposited DLC films on polymer coated-MALDI-plate for better adaptability [67].

2.4.2 Diamond Particles

The beauty of diamond is that it is available in different morphologies and forms. Diamond nanoparticles (also termed nanodiamonds) have shown high affinities for peptides and proteins through hydrophilic and hydrophobic interactions [63]. Affinity allows biological molecules in dilute solutions to be captured easily by diamond and directly measured by matrix-assisted laser desorption/ionization (MALDI) time-of flight (TOF) mass spectrometry (MS) with α-cyano-4-hydroxycinnamic acid (HCCA)

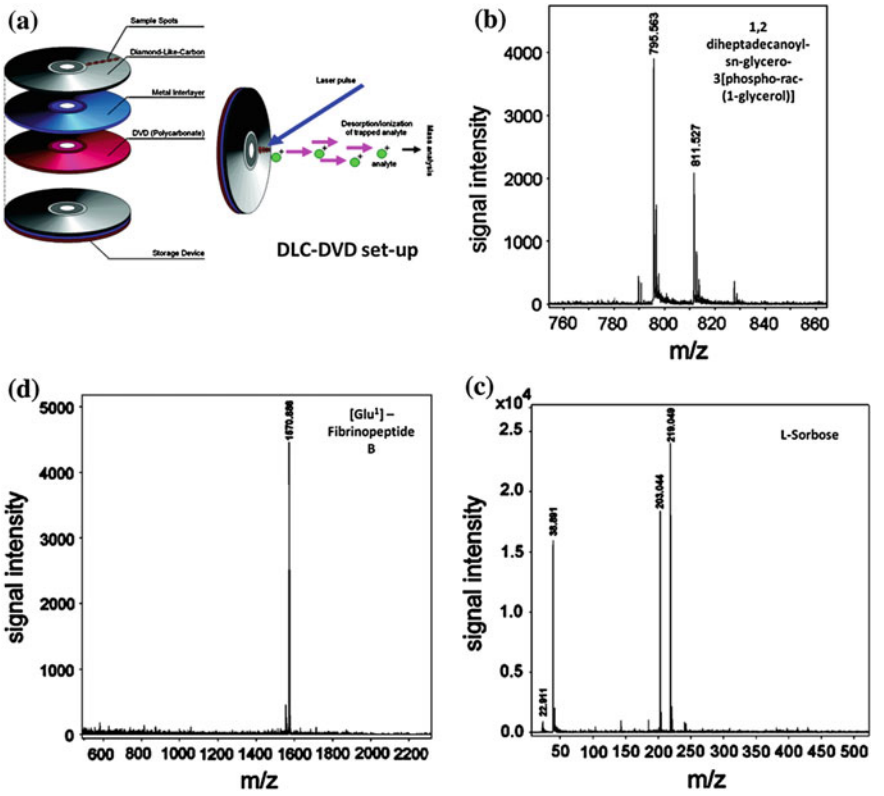

Fig. 5 DLC DVD disk set-up (**a**) developed by Najam-ul-Haq et al. for the LDI-MS detection of lipid (**b**), carbohydrate (**c**) and peptide (**d**) (reprint with permission from Najam-ul-haq et al. [14])

matrix. From 50-fold diluted human blood serum, the spectral quality was greatly improved in comparison to sample without the pre-treatment with diamond particles, with an enhancement in detection sensitivity by more than 2 orders of magnitude. Thanks to diamond particles, proteins such as cytochrome c, myoglobin, and albumin were detected at 100 pM from a 1-mL solution (Fig. 6a).

Diamond has also been utilized in solid-phase extraction (SPE), where the isolation, concentration, purification, digestion, and analysis of DNA were carried out in complex protein solutions and cell lysates [65]. Poly(L-lysine) coated carboxylated/oxidized diamond nanocrystals (100 nm in diameter) were prepared and used to isolate, concentrate, purify, and digest DNA oligonucleotides in one microcentrifuge tube for matrix-assisted laser desorption/ionization (MALDI) time of-flight (TOF) mass spectrometry. It was demonstrated that using diamond nanocrystals as a solid-phase extraction support not only permits concentration of oligonucleotides in highly diluted solutions, but also facilitates separation of oligonucleotides from proteins in heavily contaminated solutions. In addition, enzymatic digestions can be conducted on particles, and the digests can be easily

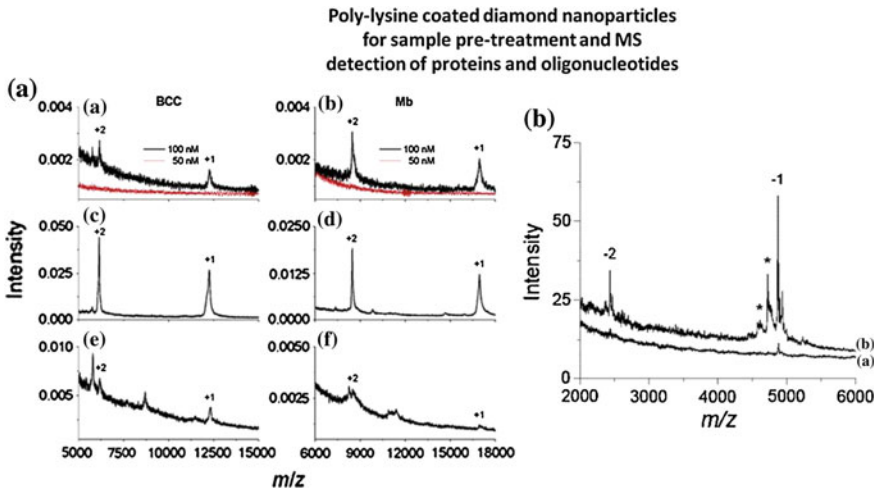

Fig. 6 Diamond nanoparticles for pre-treatment of samples containing proteins or oligonucleotides. **a** Mass spectra obtained for bovine cytochrome C (BCC) and myoglobin (Mb) without pre-treatment (*a*, *b*) and with pre-treatment with poly-lysine modified diamond particles at 50 and 0.2 nM of BCC (*c*, *e*) and Mb (*d*, *f*). **b** MS spectra of d(ATCGGCTAATCGGCTA) sequence at 10 nM without (*a*) and with pre-treatment with poly-lysine modified diamond particles (*b*). The numbers design mono-charged (*1*) and double-charged ions (*2*) of sequence and asterisks correspond to fragment ions (modified with permission from Kong et al. [63, 65])

recovered from the solution for base sequencing. A maximum adsorption of DNA molecules was observed at pH below 3. The enrichment of samples by diamond particles enhanced the ion signals detected for a 500-μL solution at 5 nM. Both singly and doubly charged ions of oligonucleotides can be clearly seen at m/z 4880 and 2440, respectively. Concentrations as low as 100 pM were measured (Fig. 6b).

2.4.3 Nanocrystalline Diamond (NCD)

Nanocrystalline diamond (NCD) can also be chemically modified as shown by Najam-ul-Haq et al. [64] using glycidyl methacrylate (GMA) under ultraviolet (UV) light. This modification was followed by the introduction of iminodiacetic acid (IDA), a chelating agent or C_{18} alkyl chain via the reaction with octadecylamine. IDA is a chelating agent, and when loaded with copper ions permits to create immobilized metal affinity chromatographic (IMAC) supports for improving sensitivity, selectivity, and capacity of detection whereas C_{18} acted as reversed phase surface [64]. Figure 7 depicts the chemical modification routes of the NCD films (IDA-Cu^{2+} and C_{18}) and the different mass spectra obtained on both surfaces for peptides and proteins profiling from serum.

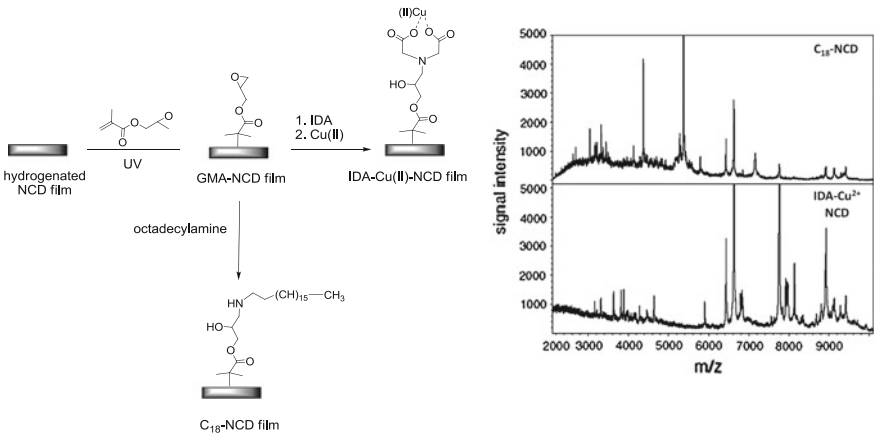

Fig. 7 NCD chemical modifications by IDA-Cu^{2+} or octadecylamine for protein and peptide mass spectrometry profiling from serum in presence of α-cyano-4-hydroxycinnamic acid (HCCA) (reprint with permission from [64])

2.4.4 Diamond Nanowires

Diamond nanowires are among the relatively new and very promising materials for chemical and biochemical sensing. The first attempt to prepare diamond nanowires dates back to 1968 using a radiation heating unit, developed from a super-high pressure Xenon lamp [68]. It was however only around the beginning of 21th century that further attempts for the synthesis of diamond nanostructures using bottom-up and top-down approaches were undertaken. While the bottom-up methods [69–74] are in general more efficient, since the growth of a thick diamond layer is time consuming and its post-processing to form nanostructures can be somehow cumbersome, only the top-down approaches are currently used for the formation of diamond nanostructures for SALDI applications [24, 75].

Top-down approaches are mainly based on the etching of CVD grown diamond films using arrays of nanoparticles seeded onto the diamond films as masks (Fig. 8a). Aluminum dots [76], SiO_2 particles [77], gold nanoparticles [78] and diamond nanoparticles [27, 29, 79, 80] showed to be useful etching masks. The choice of the material of the seeding particle is mainly governed by the possibility of depositing a uniform layer onto the CVD diamond films, the ease of forming well dispersed particle solutions, and the selectivity of etching and its rate for diamond versus metal [71]. Gold nanoparticles were found to be the most suitable seeding masks than aluminum oxide and SiO_2 nanoparticles as they are easier to disperse, resulting in single nanoparticles on the surface, requiring no further processing step.

Top-down approaches without the use of any mask have been proposed recently for the preparation of diamond nanowires [24, 75, 81–83]. Such methods have the intrinsic advantage of being simple and straightforward not requiring complicated processing steps such as mask deposition or template removal.

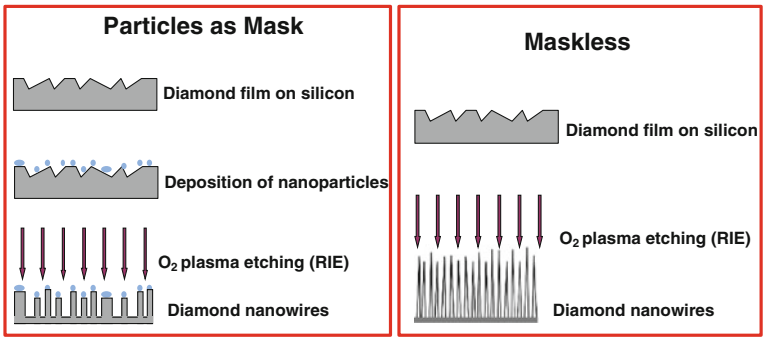

Fig. 8 Formation of diamond nanowires via reactive ion etching (RIE) using oxygen plasma with (**a**) or without (**b**) particle masking

We demonstrated that BDD nanowires can be formed from highly-doped polycrystalline diamond thin films using RIE with an oxygen plasma [24, 32, 75, 82]. Figure 9 shows some of the characterization of the formed diamond nanowires. X-ray photoelectron spectroscopy (XPS) analysis of the chemical composition of the diamond nanowires revealed that next to C_{1s} at 285 eV and O_{1s} at 532 eV, additional peaks at 402, 104 and 169 eV due to N_{1s}, Si_{2p} and S_{2p} are also present (Fig. 9a). The latter elements are believed to originate from surface contamination during the RIE process. Indeed, deposition of a SiO_x shell around the BDD NWs was confirmed by HR-TEM (Fig. 9d) and EDX analysis (Fig. 9b). SiO_x was most likely deposited during the etching process due to sputtering of the substrate holder or the silicon wafer onto which the diamond film was deposited. A similar behavior was observed by Baik et al. when Mo sample holder was used [83]. The SiO_x deposits can be easily removed in HF aqueous solutions as confirmed by XPS and EDX analysis (Fig. 9a, b). A change in nanowires morphology was in addition observed after HF treatment with sharper wires being formed thereafter (Fig. 9c).

Depending on the diamond film thickness, the resulting nanowires' dimensions can vary between 0.6 and 1.4 ± 0.1 μm in length and exhibit constant tip and base radius of r_{tip} = 10 ± 5 nm and r_{base} = 40 ± 5 nm, respectively. The wires are about 60–140 times longer than aligned diamond nanowires prepared using diamond nanoparticles as a hard mask [24, 32, 33, 75, 82]. We have also demonstrated that boron atoms are not essentially involved in the nanowires formation mechanism since undoped and doped diamond substrates led to the formation of diamond nanowires [24]. However, we have shown that the BDD film doping level can have an influence on nanowires' density (Fig. 10).

The use of diamond nanowires as a matrix-free LDI substrate for the D/I of peptides and small molecules, and their analysis by mass spectrometry with a very high sensitivity has been shown by us lately [24]. To minimize droplet spreading, the nanowires were chemically functionalized with octadecyltrichlorosilane (OTS) and then UV/ozone treated to reach a final water contact angle of 120 °C (Fig. 11a) [75]. The sub-bandgap absorption under UV laser irradiation and the heat

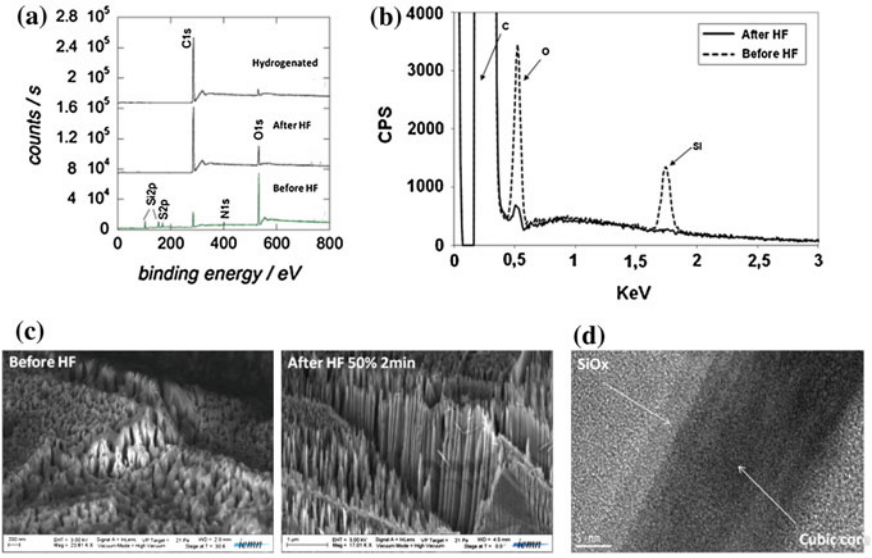

Fig. 9 **a** XPS spectra recorded on the as-prepared diamond nanowires, after HF treatment and after hydrogenation; **b** EDX spectra of the nanowires before and after HF treatment; **c** SEM images of the nanowires before and after HF treatment; **d** HR-TEM image of the as-prepared diamond nanowires [75]

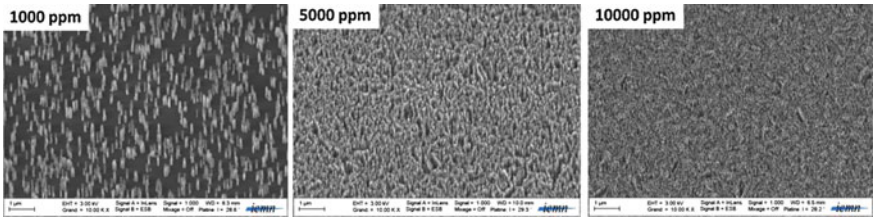

Fig. 10 Densities of diamond nanowires obtained from diamond films with different boron concentrations during the growth of BDD films (1000, 5000 and 10,000 ppm). Diamond nanowires were synthesized using O_2 plasma during 30 min at a power of 350 W, flow rate of 20 sccm O_2, pressure chamber of 150 mT (unpublished results)

confinement inside the nanowires allowed LDI-MS of various compounds, most likely via a thermal mechanism. A detection limit of 200 zeptomole for verapamil was achieved (Fig. 11b). In this study, we have observed that, for the realization of LDI-MS on such diamond surface, nanostructuration of the NCD film is required (formation of diamond nanowires). The investigated diamond nanowires, undoped (UDD) or boron-doped (BDD), display antireflective properties permitting photons absorption at $\lambda = 337$ nm (Fig. 11c, d). However, only the BDD nanowires have shown the best results in terms of LDI-MS efficiency [24].

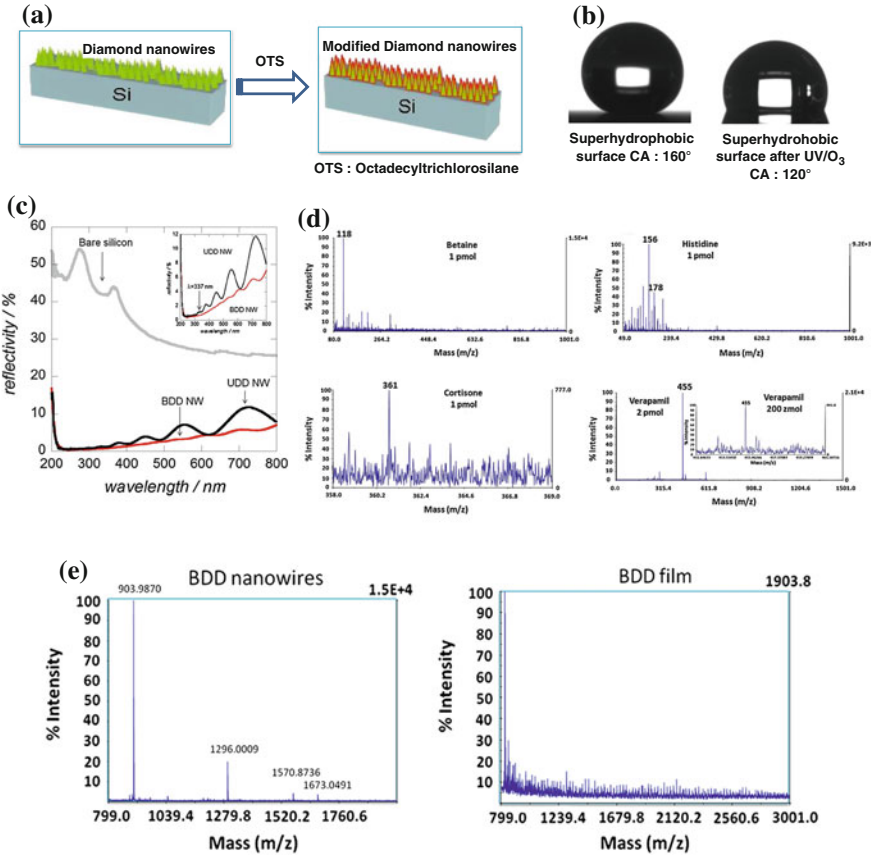

Fig. 11 Diamond nanowires for SALDI: **a** OTS modified diamond nanowires, **b** contact angle measurement before and after UV/O_3 treatment, **c** reflectivity of undoped diamond nanowires (UDD NW) and boron doped nanowires (BDD NW) compared to silicon wafer, **d** LDI-MS on BDD NW of various compounds, **e** LDI-MS detection of a peptide mixture on either BDD NW and BDD film (reprint with permission from Coffinier et al. [24])

3 Conclusion

In conclusion, different carbon nanostructures in the form of films and particle suspensions have shown to work as SALDI matrices for small molecules, peptides, proteins and other analytes. At present, most of the examples reported in the literature are based on sp^2 hybridized carbon materials. One of the drawbacks of such carbon materials as SALDI interface is the contamination of the ion source. CNTs, when used as 2D films, have the tendency to fly off into the instrument when laser pulses are applied. AB Sciex sent a note in which they specifically do not recommend the use of CNTs as matrix in any of their mass spectrometers. Attempts to overcome this limitation were undertaken such as the addition of polyurethane

adhesives to CNT matrixes [84]. The other possibility is based on the use of different matrixes.

Due to the rapid advancements made over the last years in the possibility to from sp^3 based structures in the form of diamond films, diamond nanoparticles and diamond nanowires, this material is currently considered in more detail for SALDI based applications. While there are currently only a handful of reports on the use of diamond for matrix-free mass spectrometry analysis, the encouraging results are hoped to trigger further interest of these structures for mass spectrometry based identification and quantification. A full and detailed understanding of the importance of doping level, wire length and other physical properties is needed to foster further developments in this direction. Diamond nanostructures display several advantages as SALDI substrates such as high surface area, availability (diamond nanoparticles), and ease of preparation (diamond nanowires). Moreover, the existence of numerous possibilities for integrating surface functionalities [26, 85] will allow to design chips for specific capture of analytes and their subsequent MS analysis with high sensitivity. The robust surface chemistry offered by diamond and its exceptional mechanical properties are a real asset for the reusability of the chips. Finally, the non wetting properties (superhydrophobicity) of chemically modified diamond nanowires open new opportunities for their integration in lab-on-chip devices for MS analysis [86–88]. Although diamond nanostructures are highly suitable for SALDI-MS analysis, there are some points that need special attention to make these substrates of prime interest in this field. The main hurdle is connected with the price of these substrates. Even though BDD thin films are commercially available, the price is still quite high for instance compared to silicon substrate, the starting material for the preparation of porous silicon and silicon nanowires commonly used as SALDI substrates. This can be lowered by the reutilization of the substrates. Also the preparation of BDD films of controlled doping type and level is restricted to specialized laboratories and as such limits access to these materials. However, given the promising results obtained with BDD nanowires and exceptional properties of this material, it is likely that these limitations will be overcome easily and thus make the future of diamond nanostructures for SALDI analysis an interesting challenge.

Acknowledgement The authors gratefully acknowledge financial support from the Centre National de la Recherche Scientifique (CNRS), the Université Lille 1 and the Nord Pas de Calais region.

References

1. M. Karas, F. Hillenkamp, Laser desorption ionization of proteins with molecular masses exceeding 10,000 daltons. Anal. Chem. **60**, 259–280 (1988). doi:10.1021/ac00171a028
2. S.D. Hanton, Mass spectrometry of polymers and polymer surfaces. Chem. Rev. **101**, 527–569 (2001). doi:10.1021/cr9901081

3. R. Knochenmuss, R. Zenobi, MALDI ionization: the role of in-plume processes. Chem. Rev. **103**, 441–452 (2003). doi:10.1021/cr0103773
4. L. Li, *MALDI Mass Spectrometry for Synthetic Polymer Analysis* (*Chemical Analysis: A Series of Monographs on Analytical Chemistry and Its Applications*) (Wiley-VCH, 2009). ISBN: 978–0-471-77579-9
5. K. Tanaka, H. Waki, Y. Ido, S. Akita, Y. Yoshida, T. Yoshida, Protein and polymer analyses up to m/z 100,000 by laser ionization time-of-flight mass spectrometry. Rapid Commun. Mass Spectrom. 151–153 (1988). doi:10.1002/rcm.1290020802
6. R. Arakawa, H. Kawasaki, Functionalized nanoparticles and nanostructured surfaces for surface-assisted laser desorption/ionization mass spectrometry. Anal. Sci. **26**, 1229 (2010). doi:10.2116/analsci.26.1229
7. J. Sunner, E. Dratz, Y.C. Chen, Graphite surface-assisted laser desorption/ionization time-of-flight mass spectrometry of peptides and proteins from liquid solutions. Anal. Chem. **67**, 4335–4342 (1995). doi:10.1021/ac00119a021
8. J. Wei, J.M. Buriak, G. Siuzdak, Desorption–ionization mass spectrometry on porous silicon. Nature **399**, 243–246 (1999). doi:10.1038/20400
9. J.J. Thomas, Z. Shen, J.E. Crowell, M.G. Finn, G. Siuzdak, Desorption/ionization on silicon (DIOS): a diverse mass spectrometry platform for protein characterization. Proc. Natl. Acad. Sci. USA **98**, 4932–4937 (2001). doi:10.1073/pnas.081069298
10. S.A. Trauger, E.P. Go, Z. Shen, J.V. Apon, B.J. Compton, E.S.P. Bouvier, M.G. Finn, G. Siuzdak, High sensitivity and analyte capture with desorption/ionization mass spectrometry on silylated porous silicon. Anal. Chem. **76**, 4484–4489 (2004). doi:10.1021/ac049657j
11. G. Piret, H. Drobecq, Y. Coffinier, O. Melnyk, R. Boukherroub, Matrix-free laser desorption/ionization mass spectrometry on silicon nanowire arrays prepared by chemical etching of crystalline silicon. Langmuir **26**(2), 1354–1361 (2010). doi:10.1021/la902266x
12. E.P. Go, J.V. Apon, G. Luo, A. Saghatelian, R.H. Daniels, V. Sahi, R. Dubrow, B.F. Cravatt, A. Vertes, G. Siuzdak, Desorption/ionization on silicon nanowires. Anal. Chem. **77**, 1641–1646 (2005). doi:10.1021/ac048460o
13. K.P. Law, J.R. Larkin, Recent advances in SALDI-MS techniques and their chemical and bioanalytical applications. Anal. Bioanal. Chem. **399**, 2597–2622 (2011). doi:10.1007/s00216-010-4063-3
14. M. Najam-ul-haq, M. Rainer, Z. Szabo, R. Vallant, C.W. Huck, G.K. Bonn, Role of carbon nano-materials in the analysis of biological materials by laser desorption/ionization-mass spectrometry. J. Biochem. Biophys. Methods **70**, 319–328 (2007). doi:10.1016/j.jbbm.2006.11.004
15. J.T. Shiea, J.P. Huang, C.F. Teng, J.Y. Jeng, L.Y. Wang, L.Y. Chiang, Use of a water-soluble fullerene derivative as precipitating reagent and matrix-assisted laser desorption/ionization matrix to selectively detect charged species in aqueous solutions. Anal. Chem. **75**, 3587–3595 (2003). doi:10.1021/ac020750m
16. M.J. Dale, R. Knochenmuss, R. Zenobi, Graphite/liquid mixed matrices for laser desorption/ionization mass spectrometry. Anal. Chem. **68**, 3321–3329 (1996). doi:10.1021/ac960558i
17. S. Zumbuhl, R. Knochenmuss, S. Wulfert, F. Dubois, M.J. Dale, R. Zenobi, A graphite-assisted laser desorption/ionization study of light-induced aging in triterpene dammar and mastic varnishes. Anal. Chem. **70**, 707–715 (1998). doi:10.1021/ac970574v
18. S. Xu, Y. Li, H. Zou, J. Qiu, Z. Guo, B. Guo, Carbon nanotubes as assisted matrix for laser desorption/ionization time-of-flight mass spectrometry. Anal. Chem. **75**, 6191–6195 (2003). doi:10.1021/ac0345695
19. X. Zhou, Y. Wei, Q. He, F. Boey, Q. Zhang, H. Zhang, Reduced graphene oxide films used as matrix of MALDI-TOF-MS for detection of octachlorodibenzo-p-dioxin. Chem. Commun. **46**, 6974–6976 (2010). doi:10.1039/C0CC01681K
20. Y.-K. Kim, H.-K. Na, S.-J. Kwack, S.-R. Ryoo, Y. Lee, S. Hong, S. Hong, Y. Jeong, D.-H. Min, Synergistic effect of graphene oxide/MWCNT films in laser desorption/ionization mass

spectrometry of small molecules and tissue imaging. ACS Nano **5**, 4550–4561 (2011). doi:10.1021/nn200245v
21. M.V. Ugarov, T. Egan, D.V. Khabashesku, J.A. Schultz, H. Peng, V.N. Khabashesku, H. Furutani, K.S. Prather, H.W.J. Wang, S.N. Jackson, A.S. Woods, MALDI matrices for biomolecular analysis based on functionalized carbon nanomaterials. Anal. Chem. **76**, 6734–6742 (2004). doi:10.1021/ac049192x
22. C. Pan, S. Xu, L. Hu, X. Su, J. Ou, H. Zou, Z. Guo, Y. Zhang, B. Guo, Using oxidized carbon nanotubes as matrix for analysis of small molecules by MALDI-TOF MS. J. Am. Soc. Mass Spectrom. **16**, 883–892 (2005). doi:10.1016/j.jasms.2005.03.009
23. S.F. Ren, Y.L. Guo, Oxidized carbon nanotubes as matrix for matrix-assisted laser desorption/ionization time-of-flight mass spectrometric analysis of biomolecules. Rapid Commun. Mass Spectrom. **19**, 255–260 (2005). doi:10.1002/rcm.1779
24. Y. Coffinier, S. Szunerits, H. Drobecq, O. Melnyk, R. Boukherroub, Diamond nanowires for highly sensitive matrix-free mass spectrometry analysis of small molecules. Nanoscale **4**, 231–238 (2012). doi:10.1039/C1NR11274K
25. Y. Yu, L. Wu, J. Zhi, Diamond nanowires: fabrication, structure, properties, and applications. Angew. Chem. Int. Ed. **53**, 14326–14351 (2014). doi:10.1002/anie.201310803
26. S. Szunerits, R. Boukherroub, Different strategies for chemical functionalization of diamond surfaces. J. Solid-State Electrochem. **12**, 1205–1218 (2008). doi:10.1007/s10008-007-0473-3
27. N. Yang, H. Uetsuka, E. Osawa, C.E. Nebel, Vertically aligned diamond nanowires for DNA sensing. Angew. Chem. Int. Ed. **47**, 5183–5185 (2008). doi:10.1002/anie.200801706
28. H. Uetsuka, D. Shin, N. Tokuda, K. Saeki, C.E. Nebel, Electrochemical grafting of boron-doped single-crystalline chemical vapor deposition diamond with nitrophenyl molecules. Langmuir **23**, 3466–3472 (2007). doi:10.1021/la063241e
29. C.E. Nebel, N. Yang, H. Uetsuka, E. Osawa, N. Tokuda, O. Williams, Diamond nano-wires, a new approach towards next generation electrochemical gene sensor platforms. Diamond Relat. Mater. **18**, 910 (2009). doi:10.1016/j.diamond.2008.11.024
30. N. Yang, W. Smirnov, C.E. Nebel, Three-dimensional electrochemical reactions on tip-coated diamond nanowires with nickel nanoparticles. Electrochem. Commun. **27**, 89–91 (2013). doi:10.1016/j.elecom.2012.10.044
31. D. Luo, L. Wu, J. Zhi, Fabrication of boron-doped diamond nanorod forest electrodes and their application in nonenzymatic amperometric glucose sensing. ACS Nano **3**, 2121–2128 (2009). doi:10.1021/nn9003154
32. Q. Wang, P. Subramanian, M. Li, W.S. Yeap, K. Haenen, Y. Coffinier, R. Boukherroub, S. Szunerits, Non-enzymatic glucose sensing on long and short diamond nanowires electrodes. Electrochem. Commun. **34**, 286–290 (2013). doi:10.1016/j.elecom.2013.07.014
33. Q. Wang, A. Vasilescu, P. Subramanian, V. Andrei, Y. Coffinier, M. Li, R. Boukherroub, S. Szunerits, Simultaneous electrochemical detection of tryptophan and tyrosine using boron-doped diamond and diamond nanowires electrodes. Electrochem. Commun. **35**, 84–87 (2013). doi:10.1016/j.elecom.2013.08.010
34. S. Szunerits, Y. Coffinier, E. Galopin, J. Brenner, R. Boukherroub, Preparation of boron-doped diamond nanowires and their application for sensitive electrochemical detection of tryptophan. Electrochem. Commun. **12**, 438 (2010). doi:10.1016/j.elecom.2010.01.014
35. P. Subramanian, I. Mazurenko, V. Zaitsev, Y. Coffinier, R. Boukherroub, S. Szunerits, Diamond nanowires modified with poly[3-(pyrrolyl)carboxylic acid] for the immobilization of histidine-tagged peptides. Analyst **139**, 4343–4349 (2014). doi:10.1039/c4an00146j
36. P. Subramanian, J. Foord, D. Steinmueller, Y. Coffinier, R. Boukherroub, S. Szunerits, Diamond nanowires decorated with metallic nanoparticles: a novel electrical interface for the immobilization of histidinylated biomolecules. Electrochim. Acta **110**, 4–8 (2013). doi:10.1016/j.electacta.2012.11.010
37. P. Subramanian, A. Motorina, W.S. Yeap, K. Haenen, Y. Coffinier, V. Zaitsev, J. Niedziolka-Jonsson, R. Boukherroub, S. Szunerits, Impedimetric immunosensor based on diamond nanowires decorated with nickel nanoparticles. Analyst **139**, 1726–1731 (2014). doi:10.1039/c3an02045b

38. S. Szunerits, Y. Coffinier, R. Boukherroub, Diamond nanowires: a recent success story for biosensing. In: *Nanosensor Technology*. Springer Series on Chemical Sensors and Biosensors (Springer, Heidelberg, 2015) (in print)
39. Y.C. Chen, J. Shiea, J. Sunner, Thin-layer chromatography–mass spectrometry using activated carbon, surface-assisted laser desorption/ionization. J. Chromatogr. A **826**, 77–86 (1998). doi:10.1016/S0021-9673(98)00726-2
40. H.J. Kim, J.K. Lee, S.J. Park, H.W. Ro, D.Y. Yoo, D.Y. Yoon, Observation of low molecular weight poly(methylsilsesquioxane)s by graphite plate laser desorption/ionization time-of-flight mass spectrometry. Anal. Chem. **72**, 5673–5678 (2000). doi:10.1021/ac0003899
41. K.H. Park, H.J. Kim, Analysis of fatty acid by graphite plate laser desorption/ionization time of flight mass spectrometry. Rapid Commun. Mass Spectrom. **15**, 1494–1499 (2001). doi:10.1002/rcm.387
42. J. Kim, K. Paek, W. Kang, Visible surface-assisted laser desorption/ ionization mass spectrometry of small macromolecules deposited on the graphite plate. Bull. Korean Chem. Soc. **23**, 315–319 (2002). doi:10.1002/pmic.200401023
43. Y.C. Chen, J.Y. Wu, Analysis of small organics on planar silica surfaces using surface-assisted laser desorption/ionization mass spectrometry. Rapid Commun. Mass Spectrom. **20**, 1899–1903 (2001). doi:10.1002/rcm.451
44. C. Black, C. Poile, J. Langley, J. Herniman, The use of pencil lead as a matrix and calibrant for matrix-assisted laser desorption/ionisation. Rapid Commun. Mass Spectrom. **20**, 1053–1060 (2006). doi:10.1002/rcm.2408
45. S. Cha, E.S. Yeung, Colloidal graphite-assisted laser desorption/ionization mass spectrometry and MSn of small molecules. 1. Imaging of cerebosides directly from rat brain tissue. Anal. Chem. **79**, 2373–2385 (2007). doi:10.1021/ac062251h
46. S. Cha, H. Zhang, H.I. Ilarsaln, Z.S. Wurtele, L. Brachova, B.J. Nikolau, E.S. Yeung, Direct profiling and imaging of plant metabolites in intact tissues by using colloidal graphite-assisted laser desorption ionization mass spectrometry. Plant. J. **55**, 348–360 (2008). doi:10.1111/j.1365-313X.2008.03507
47. H. Zhang, S. Cha, E.S. Yeung, Colloidal graphite-assisted laser desorption/ionization MS and MS n of small molecules. 2. Direct profiling and MS imaging of small metabolites from fruits. Anal. Chem. **79**, 6575–6584 (2007). doi:10.1021/ac0706170
48. H. Kawasaki, T. Takahashi, F. Fujimori, O. Okumura, W. Watanabe, M. Matsumura, T. Takemine, T. Nakano, R. Arakawa, Functionalized pyrolytic highly oriented graphite polymer film for surface-assisted laser desorption/ ionization mass spectrometry in environmental analysis. Rapid Commun. Mass Spectrom. **23**, 3323–3332 (2009). doi:10.1002/rcm.4254
49. M. Najam-ul-haq, M. Rainer, T. Schwarzenauer, C.W. Huck, G.K. Bonn, Chemically modified carbon nanotubes as material enhanced laser desorption ionisation (MELDI) material in protein profiling. Anal. Chim. Acta **561**, 32–39 (2006). doi:10.1016/j.aca.2006.01.012
50. W.Y. Chen, L.S. Wang, H.T. Chiu, Y.C. Chen, C.Y. Lee, Carbon nanotubes as affinity probes for peptides and proteins in MALDI MS analysis. J. Am. Soc. Mass Spectrom. **15**, 629–635 (2004). doi:10.1016/j.jasms.2004.08.001
51. L.-S. Wang, C.-Y. Lee, H.-T. Chiu, New nanotube synthesis strategy—application of sodium nanotubes formed inside anodic aluminium oxide as a reactive template. Chem. Commun. **15**, 1964–1965 (2003). doi:10.1039/B305610D
52. C.-T. Chen, Y.-C. Chen, Desorption/ionization mass spectrometry on nanocrystalline titania sol–gel-deposited films. Rapid Commun. Mass Spectrom. **18**, 1956–1964 (2004). doi:10.1002/rcm.1572
53. C. Pan, S. Xu, H. Zou, Z. Guo, Y. Zhang, B. Guo, Carbon nanotubes as adsorbent of solid-phase extraction and matrix for laser desorption/ ionization mass spectrometry. J. Am. Soc. Mass Spectrom. **16**, 263–270 (2005). doi:10.1016/j.jasms.2004.11.005
54. J. Zhang, H.Y. Wang, Y.L. Guo, Amino acids analysis by MALDI mass spectrometry using carbon nanotube as matrix. Chin. J. Chem. **23**, 185–189 (2005)

55. E. Nakamura, H. Isobe, Functionalized fullerenes in water. The first 10 years of their chemistry, biology, and nanoscience. Acc. Chem. Res. **36**, 807–815 (2003). doi:10.1021/ar030027y
56. F.G. Hopwood, L. Michalak, D.S. Alderdice, K.J. Fisher, G.D. Willet, C_{60}-assisted laser desorption/ionization mass spectrometry in the analysis of phospho tungstic acid. Rapid Commun. Mass Spectrom. **8**, 881–885 (1994). doi:10.1002/rcm.1290081105
57. Y.H. Lee, J.W. Shin, S. Ryu, S.W. Lee, C.H. Lee, K. Lee, Enrichment of N-terminal sulfonated peptides by water-soluble fullerene derivative and its applications to highly efficient proteomics. Anal. Chim. Acta 556, 140–144 (2006). doi:10.1016/j.aca.2005.06.060
58. R.M. Vallant, Z. Szabo, L. Trojer, M. Najam-ul-Haq, M. Rainer, C.W. Huck, R. Bakry, G.K. Bonn, A new analytical approach for the determination of low mass serum constituents employing fullerene derivatives for selective enrichment. J. Proteome Res. **6**, 44–53 (2007). doi:10.1021/pr060347m
59. X. Chen, L. Hu, X. Su, L. Kong, M. Ye, H. Zou, Separation and detection of compounds in Honeysuckle by integration of ion-exchange chromatography fractionation with reversed-phase liquid chromatography-atmospheric pressure chemical ionization mass spectrometer and matrix-assisted laser desorption/ionization time-of-flight mass spectrometry analysis. J. Pharm. Biomed. Anal. **40**, 559–570 (2006). doi:10.1016/j.jpba.2005.07.043
60. X. Chen, L. Kong, X. Su, C. Pan, M. Ye, H. Zou, Integration of ion-exchange chromatography fractionation with reversed-phase liquid chromatography atmospheric pressure chemical ionization mass spectrometer and matrix assisted laser desorption/ionization time-of-flight mass spectrometry for isolation and identification of compounds in *Psoralea corylifolia*. J. Chromatogr. A **1089**, 87–100 (2005). doi:10.1016/j.chroma.2005.06.067
61. L. Hu, S. Xu, C. Pan, C. Yuan, H. Zou, G. Jiang, Matrix-assisted laser desorption/ionization time-of-flight mass spectrometry with a matrix of carbon nanotubes for the analysis of low-mass compounds in environmental samples. Environ. Sci. Technol. **39**, 8442–8447 (2005). doi:10.1021/es0508572
62. M. Rainer, M.N. Quershi, G.K. Bonn, Matrix-free and material-enhanced laser desorption/ionization mass spectrometry for the analysis of low molecular weight compounds. Anal. Bioanal. Chem. **400**, 2281–2288 (2011). doi:10.1007/s00216-010-4138-1
63. X.L. Kong, L.C.L. Huang, C.M. Hsu, W.H. Chen, C.C. Han, H.C. Chang, High affinity capture of proteins by diamond nanoparticles for mass spectrometric analysis. Anal. Chem. **77**, 259–265 (2005). doi:10.1021/ac048971a
64. M. Najam-ul-Haq, M. Rainer, C.W. Huck, G. Stecher, I. Feuerstein, D. Steinmueller, G.K. Bonn, Chemically modified nano crystalline diamond layer as material enhanced laser desorption ionisation (MELDI) surface in protein profiling. Curr. Nanosci. **2**, 1–7 (2006). doi:10.2174/157341306775473836
65. X.L. Kong, L.C.L. Huang, S.C.V. Liau, C.C. Han, H.C. Chang, Polylysine-coated diamond nanocrystals for MALDI-TOF mass analysis of DNA oligonucleotides. Anal. Chem. **77**, 4273–4277 (2005). doi:10.1021/ac050213c
66. L. Sage, Femtomolar sensitivity with matrix-free LDI MS. Anal. Chem. **80**, 5515–5523 (2008). doi:10.1021/ac801668w
67. W. Winkler, W. Balika, P. Hausberger, H. Kraushaar, G. Allmaier, Diamond-like diamond coated polymer-based target in microscope slide format for MALDI mass spectrometry. J. Mass Spectrom. **45**, 566–569 (2010). doi:10.1002/jms.1744
68. B.V. Derjaguin, D.V. Fedoseev, V.M. Lukyanovich, B.V. Spitzin, V.A. Ryabov, A.V. Lavrentyev, Filamentary diamond crystals. J. Cryst. Growth **2**, 380–384 (1968). doi:10.1016/0022-0248(68)90033-X
69. N. Shang, P. Papakonstantinou, P. Wang, A. Zakharov, U. Palnitkar, I.N. Lin, M. Chu, A. Stamboulis, Self-assembled growth, microstructure, and field-emission high-performance of ultrathin diamond nanorods. ACS Nano **3**, 1032–1038 (2009). doi:10.1021/nn900167p
70. C.-H. Hsu, J. Xu, Diamond nanowire—a challenge from extremes. Nanoscale **4**, 5293 (2012). doi:10.1039/c2nr31260c

71. B.J.M. Hausmann, M. Khan, Y. Zhang, T.M. Bainec, K. Martinick, M. McCutcheon, P. Hemmer, M. Loncar, Fabrication of diamond nanowires for quantum information processing applications. Diamond Relat. Mater. **19**, 621–629 (2010). doi:10.1016/j.diamond.2010.01.011
72. H. Masuda, M. Watanaba, K. Yasui, D. Tryk, T. Rao, A. Fujishima, Fabrication of a nanostructured diamond honeycomb film. Adv. Mater. **12**, 444–447 (2000). doi:10.1002/(SICI)1521-4095(200003)12:63.3.CO;2-B
73. T.M. Babinec, B.J.M. Hausmann, M. Khan, Y. Zhang, J.R. Maze, P.R. Hemmer, M. Loncar, A diamond nanowire single-photon source. Nat. Nanotechnol. **5**, 195–199 (2010). doi:10.1038/nnano.2010.6
74. H. Masuda, T. Yanagishita, K. Yasui, K. Nishio, I. Yagi, N. Rao, A. Fujishima, Synthesis of well-aligned diamond nanocylinders. Adv. Mater. **13**, 247 (2001). doi:10.1002/1521-4095(200102)13:4<247:AID-ADMA247>3.0.CO;2-H
75. Y. Coffinier, E. Galopin, S. Szunerits, R. Boukherroub, Preparation of superhydrophobic and oleophobic diamond nanograss array. J. Mater. Chem. **20**, 10671–10675 (2010). doi:10.1039/C0JM01296C
76. Y. Ando, Y. Nishibayashi, A. Sawaben, 'Nano-rods' of single crystalline diamond. Diamond Relat. Mater. **13**, 633 (2004). doi:10.1016/j.diamond.2003.10.066
77. S. Okuyama, S.I. Matsushita, A. Fujishima, Periodic submicrocylinder diamond surfaces using two-dimensional fine particle arrays. Langmuir **18**, 8282–8287 (2002). doi:10.1021/la011107i
78. Y.S. Zou, T. Yang, W.J. Zhang, Y.M. Chong, B. He, I. Bello, S.T. Lee, Fabrication of diamond nanopillar and their arrays. Appl. Phys. Lett. **92**, 053105 (2008). doi:10.1063/1.2841822
79. N. Yang, H. Uetsuka, E. Osawa, C.E. Nebel, Vertically aligned nanowires from boron-doped diamond. Nano Lett. **8**, 3572–3576 (2008). doi:10.1021/nl801136h
80. W. Smirnov, A. Kriele, N. Yang, C.F. Nebel, Aligned diamond nano-wires: fabrication and characterisation for advanced applications in bio and electrochemistry. Diamond Relat. Mater. **18**, 186–189 (2009). doi:10.1016/j.diamond.2009.09.001
81. M. Wei, C. Terashima, M. Lv, A. Fujishima, Z.-Z. Gu, Boron-doped diamond nanograss array for electrochemical sensors. Chem. Commun. 3624 (2009). doi:10.1039/B903284C
82. S. Szunerits, Y. Coffinier, E. Galopin, J. Brenner, R. Boukherroub, Preparation of boron-doped diamond nanowires and their application for sensitive electrochemical detection of tryptophan. Electrochem. Commun. **12**, 438–441 (2010). doi:10.1016/j.elecom.2010.01.014
83. E.-S. Baik, Y.-J. Baik, D. Jeaon, Aligned diamond nanowhiskers. J. Mater. Res. **15**, 923 (2000). doi:10.1557/JMR.2000.0131
84. S.F. Ren, L. Zhang, Z.H. Cheng, Y.L. Guo, Immobilized carbon nanotubes as matrix for MALDI-TOF-MS analysis: applications to neutral small carbohydrates. J. Am. Soc. Mass Spectrom. **16**, 333–339 (2005). doi:10.1016/j.jasms.2004.11.017
85. S. Szunerits, C.E. Nebel, R.J. Hamers, Surface functionalization and biological applications of CVD diamond. MRS Bull. **309**(6), 517–524 (2014). doi:10.1557/mrs.2014.99
86. F. Lapierre, G. Piret, H. Drobecq, O. Melnyk, Y. Coffinier, V. Thomy, R. Boukherroub, High sensitive matrix-free mass spectrometry analysis of peptides using silicon nanowires-based digital microfluidic device. Lab Chip **11**, 1620–1628 (2011). doi:10.1039/c0lc00716a
87. M. Jönsson-Niedziolka, F. Lapierre, Y. Coffinier, S.J. Parry, F. Zoueshtiagh, T. Foat, V. Thomy, R. Boukherroub, EWOD driven cleaning of bioparticles on hydrophobic and superhydrophobic surfaces. Lab Chip **11**, 490–496 (2011). doi:10.1039/c0lc00203h
88. F. Lapierre, M. Harnois, Y. Coffinier, R. Boukherroub, V. Thomy, Split and flow: reconfigurable capillary connection for digital microfluidic systems. Lab Chip **14**, 3589–3593 (2014). doi:10.1039/c4lc00650j